12

Electronic Energy Levels in a Cubic Crystal

In this chapter we apply space groups to determine the electronic dispersion relations in crystalline materials, and use as an illustration the symmetrized plane wave solutions of a cubic crystal.

12.1 Introduction

Suppose that we wish to calculate the electronic energy levels of a solid from a specified potential. There are many techniques available for this purpose. Some techniques are based on what is called first principles *ab initio* calculations and directly find solutions to Schrödinger's equation. Others are based on the symmetry-imposed form of the dispersion relations, which are used to fit experimental data. In all cases these techniques utilize the *spacial symmetry of the crystal*, and emphasize the electronic energy bands at high symmetry points and along high symmetry axes in the Brillouin zone.

To illustrate how group theory is utilized in these calculations, we will consider explicitly the energy bands of the nearly free electron model because of its pedagogic value. If there were no periodic potential, the energy eigenvalues would be the free electron energies

$$E(\boldsymbol{k'}) = \frac{\hbar^2 k'^2}{2m}\,, \quad V(\boldsymbol{r}) = 0\,, \tag{12.1}$$

and the free electron eigenfunctions would be

$$\psi_{k'}(\boldsymbol{r}) = \frac{1}{\sqrt{\Omega}} \mathrm{e}^{\mathrm{i}\boldsymbol{k'}\cdot\boldsymbol{r}}\,, \tag{12.2}$$

where $\boldsymbol{k'}$ is a wave vector in the extended Brillouin zone and Ω is the volume of the crystal. In the empty lattice model, the presence of a weak periodic potential imposes the symmetry of the crystal on the "empty lattice" electronic energy bands, but the potential $V(\boldsymbol{r})$ itself is considered in the limit

$V(\boldsymbol{r}) \to 0$. From a group theoretical point of view, the *free electron energy bands correspond to the symmetry of the full rotation group and the weak periodic potential serves to lower the symmetry* to that of the crystalline solid, as for example to O_h^1 (space group #221) symmetry for a simple cubic crystal. Thus, the introduction of a periodic potential results in symmetry-lowering, similar to the crystal field problem (Sect. 5.3) which we have by now encountered in several contexts. We consider the empty lattice energy bands in the reduced zone by writing the wave vector $\boldsymbol{k'}$ in the extended zone scheme as

$$\boldsymbol{k'} = \boldsymbol{k} + \boldsymbol{K}_{n_i}\,, \tag{12.3}$$

where $\boldsymbol{k}$ is a reduced wave vector in the first Brillouin zone and $\boldsymbol{K}_{n_i}$ is a reciprocal lattice vector to obtain

$$E(\boldsymbol{k} + \boldsymbol{K}_{n_i}) = \frac{\hbar^2}{2m}(\boldsymbol{k} + \boldsymbol{K}_{n_i}) \cdot (\boldsymbol{k} + \boldsymbol{K}_{n_i})\,, \tag{12.4}$$

where

$$\boldsymbol{K}_{n_i} = \frac{2\pi}{a}(n_1, n_2, n_3)\,, \quad \text{and} \quad n_i = \text{integer}\,, \quad i = 1, 2, 3\,. \tag{12.5}$$

We use the subscript $\boldsymbol{K}_{n_i}$ on the energy eigenvalues E_{n_i} to denote the pertinent $\boldsymbol{K}_{n_i}$ vector when using the wave vector $\boldsymbol{k}$ within the first Brillouin zone. If we write $\boldsymbol{k}$ in dimensionless units

$$\boldsymbol{\xi} = \frac{\boldsymbol{k}a}{2\pi}\,, \tag{12.6}$$

we obtain

$$E_{\boldsymbol{K}_{n_i}}(\boldsymbol{k}) = \frac{\hbar^2}{2m}\left(\frac{2\pi}{a}\right)^2 \left[(\xi_1 + n_1)^2 + (\xi_2 + n_2)^2 + (\xi_3 + n_3)^2\right]\,. \tag{12.7}$$

The empty lattice energy bands for the FCC cubic structure are shown in Fig. 12.1 at the high symmetry points and along the high symmetry directions indicated by the Brillouin zone for the FCC lattice (see Fig. C.5a in Appendix C). The energy bands are labeled by the symmetries of the irreducible representations appropriate to the group of the wave vector corresponding to the pertinent space group. Group theory provides us with the symmetry designations and with the level degeneracies. In Sect. 12.2, we treat the symmetry designations and mode degeneracies for the simple cubic lattice at $\boldsymbol{k} = 0$, and in Sects. 12.3 and 12.4 at other symmetry points in the Brillouin zone. In Sect. 12.5, the effect of screw axes and glide planes on the electronic energy band structure is considered.

In the reduced zone scheme, the wave functions for the plane wave solutions to the empty lattice model become the Bloch functions

$$\psi_{\boldsymbol{k'}}(\boldsymbol{r}) = \frac{1}{\sqrt{\Omega}}\mathrm{e}^{\mathrm{i}\boldsymbol{k'}\cdot\boldsymbol{r}} = \frac{1}{\sqrt{\Omega}}\mathrm{e}^{\mathrm{i}\boldsymbol{k}\cdot\boldsymbol{r}}\mathrm{e}^{\mathrm{i}\boldsymbol{K}_{n_i}\cdot\boldsymbol{r}}\,, \tag{12.8}$$

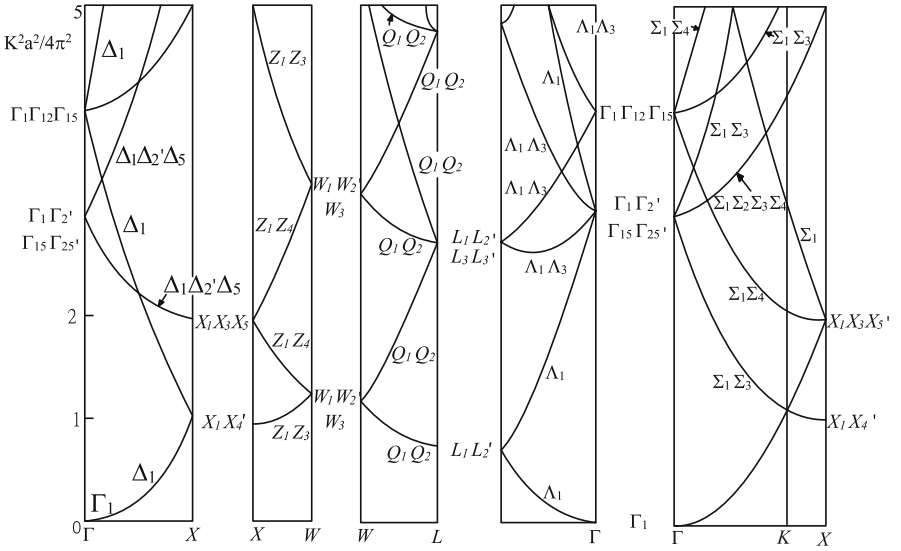

Fig. 12.1. Free-electron bands of the empty lattice in a face centered cubic structure. The labels of the high symmetry points in the FCC structure are given in Fig. C.5(a) of Appendix C. The band degeneracies can be obtained from the dimensions of the irreducible representations indicated on this diagram, and the energy is given in units of $(\hbar^2/2\mathrm{m})(2\pi/\mathrm{a})^2$

where the periodic part of the Bloch function is written as

$$u_{\boldsymbol{k}}(\boldsymbol{r}) = \mathrm{e}^{\mathrm{i}\boldsymbol{K}_{n_i}\cdot\boldsymbol{r}}\,. \tag{12.9}$$

According to Bloch's theorem, the effect of the lattice vector translation operator $\{\varepsilon|\boldsymbol{R}_n\}$ is to introduce a phase factor

$$\{\varepsilon|\boldsymbol{R}_n\}\psi_{\boldsymbol{k}}(\boldsymbol{r}) = \mathrm{e}^{\mathrm{i}\boldsymbol{k}\cdot\boldsymbol{R}_n}\psi_{\boldsymbol{k}}(\boldsymbol{r})\,, \tag{12.10}$$

$\mathrm{e}^{\mathrm{i}\boldsymbol{k}\cdot\boldsymbol{R}_n}$ involving the lattice vector $\boldsymbol{R}_n$.

In calculating the electronic energy bands in the empty lattice approximation, we recognize that the main effect of the periodic potential $V(\boldsymbol{r})$ in the limit $V(\boldsymbol{r}) \to 0$ limit is to lift the degeneracy of $E_{\boldsymbol{K}_{n_i}}(\boldsymbol{k})$. At certain high symmetry points or axes and at the Brillouin zone boundary, the degeneracy in many cases is not fully lifted in the $V(\boldsymbol{r}) \to 0$ limit and a finite periodic potential is needed to lift the degeneracy of the empty lattice dispersion relations. Group theory tells us the form of the interactions, the symmetry of the levels and their degeneracies. For each of the high symmetry points in the Brillouin zone, different symmetry operations will be applicable, depending on the appropriate group of the wave vector for the $\boldsymbol{k}$ point under consideration, as illustrated below.

12.2 Plane Wave Solutions at $\boldsymbol{k} = 0$

The highest symmetry point in the Brillouin zone is of course the Γ point ($\boldsymbol{k} = 0$) and we will therefore first illustrate the application of group theoretical considerations to the energy bands at the Γ point first for a cubic crystal. Setting $\boldsymbol{k} = 0$ in (12.7), the energy eigenvalue $E_{\boldsymbol{K}_{n_i}}(\boldsymbol{k})$ becomes

$$E_{\boldsymbol{K}_{n_i}}(0) = \frac{\hbar^2}{2m}\left(\frac{2\pi}{a}\right)^2 \left[n_1^2 + n_2^2 + n_3^2\right] = \frac{\hbar^2}{2m}\left(\frac{2\pi}{a}\right)^2 N^2\,, \tag{12.11}$$

where

$$N^2 = n_1^2 + n_2^2 + n_3^2\,. \tag{12.12}$$

Corresponding to each reciprocal lattice vector $\boldsymbol{K}_{n_i}$, a value for $E_{\boldsymbol{K}_{n_i}}(0)$ is obtained. For most $\boldsymbol{K}_{n_i}$ vectors, these energies are degenerate. We will now enumerate for illustrative purposes the degeneracy of the first few levels, starting with $\boldsymbol{K}_{n_i} = 0$ and $n_1 = n_2 = n_3 = 0$. We then find which irreducible representations for O_h are contained in each degenerate state. If then a periodic potential is applied, the degeneracy of some of these levels will be lifted. Group theory provides a powerful tool for specifying how these degeneracies are lifted. In Table 12.1 we give the energy, the degeneracy and the set of $\boldsymbol{K}_{n_i}$ vectors that yield each of the five lowest energy eigenvalues $E_{\boldsymbol{K}_{n_i}}(0)$ in cubic symmetry. The example that we explicitly work out here is for the simple cubic lattice [space group #221 (O_h^1) or $Pm3m$], and many of the pertinent character tables are found in Appendix C.

At $\boldsymbol{K}_{n_i} = 0$ we have $\psi_{\boldsymbol{k}}(\boldsymbol{r}) = (1/\sqrt{\Omega})\mathrm{e}^{\mathrm{i}\boldsymbol{k}\cdot\boldsymbol{r}}$. For a general $\boldsymbol{K}_{n_i}$ vector, (n_1, n_2, n_3) there will in general be a multiplicity of states with the same energy. We now show how to choose a properly symmetrized combination of plane waves which transform as irreducible representations of the group of the wave vector at $\boldsymbol{k} = 0$, and therefore bring the empty lattice Hamiltonian into block diagonal form. In the presence of a weak cubic periodic potential $V(\boldsymbol{r})$, the degeneracy of states which transform as different irreducible representations will be partially lifted.

By calculating the characters for the equivalence transformation, we obtain $\chi^{\text{equiv.}}$ which is used to project out the irreducible representations contained in $\Gamma^{\text{equiv.}}$. We can then specify which plane waves are transformed into one another by the elements of the group of the wave vector at the Γ point ($\boldsymbol{k} = 0$). From $\Gamma^{\text{equiv.}}$, we can find the irreducible representations of O_h which correspond to each empty lattice energy state and we can furthermore find the appropriate linear combination of plane wave states which correspond to a particular irreducible representation of O_h.

To calculate $\Gamma^{\text{equiv.}}$, we use the diagram in Fig. 12.2 which shows the cubic symmetry operations of point group O_h. The character table for O_h symmetry is given in Table 10.2 (see also Table A.30), where the column on the left gives the familiar solid state notation for the irreducible representations of O_h. In calculating $\chi^{\text{equiv.}}$ we consider that if a given plane wave goes into itself under

Table 12.1. Listing of the energy, degeneracy and the list of $\boldsymbol{K}_{n_i}$ vectors for the five lowest energy levels for the simple cubic lattice at $\boldsymbol{k} = 0$

(i)	$E_{\{000\}}(0) = 0$	degeneracy=1	$\boldsymbol{K}_{n_{\{000\}}} = 0$	(0,0,0)	$N^2 = 0$
(ii)	$E_{\{100\}}(0) = \frac{\hbar^2}{2m}\left(\frac{2\pi}{a}\right)^2$	degeneracy=6	$\boldsymbol{K}_{n_{\{100\}}} = \frac{2\pi}{a}$	$\begin{cases}(1,0,0)\\(\bar{1},0,0)\\(0,1,0)\\(0,\bar{1},0)\\(0,0,1)\\(0,0,\bar{1})\end{cases}$	$N^2 = 1$
Plane Wave States: $\mathrm{e}^{\pm\frac{2\pi \mathrm{i} x}{a}}, \mathrm{e}^{\pm\frac{2\pi \mathrm{i} y}{a}}, \mathrm{e}^{\pm\frac{2\pi \mathrm{i} z}{a}}$					
(iii)	$E_{\{110\}}(0) = 2\frac{\hbar^2}{2m}\left(\frac{2\pi}{a}\right)^2$	degeneracy=12	$\boldsymbol{K}_{n_{\{110\}}} = \frac{2\sqrt{2}\pi}{a}$	$\begin{cases}(1,1,0)\\(\bar{1},1,0)\\(1,0,1)\\(\bar{1},0,1)\\(0,1,1)\\(0,\bar{1},1)\\(1,\bar{1},0)\\(\bar{1},\bar{1},0)\\(1,0,\bar{1})\\(\bar{1},0,\bar{1})\\(0,1,\bar{1})\\(0,\bar{1},\bar{1})\end{cases}$	$N^2 = 2$
(iv)	$E_{\{111\}}(0) = 3\frac{\hbar^2}{2m}\left(\frac{2\pi}{a}\right)^2$	degeneracy=8	$\boldsymbol{K}_{n_{\{111\}}} = \frac{2\sqrt{3}\pi}{a}$	$\begin{cases}(1,1,1)\\(1,\bar{1},1)\\(1,1,\bar{1})\\(\bar{1},1,1)\\(\bar{1},\bar{1},1)\\(1,\bar{1},\bar{1})\\(\bar{1},1,\bar{1})\\(\bar{1},\bar{1},\bar{1})\end{cases}$	$N^2 = 3$
(v)	$E_{\{200\}}(0) = 4\frac{\hbar^2}{2m}\left(\frac{2\pi}{a}\right)^2$	degeneracy=6	$\boldsymbol{K}_{n_{\{200\}}} = \frac{4\pi}{a}$	$\begin{cases}(2,0,0)\\(\bar{2},0,0)\\(0,2,0)\\(0,\bar{2},0)\\(0,0,2)\\(0,0,\bar{2})\end{cases}$	$N^2 = 4$

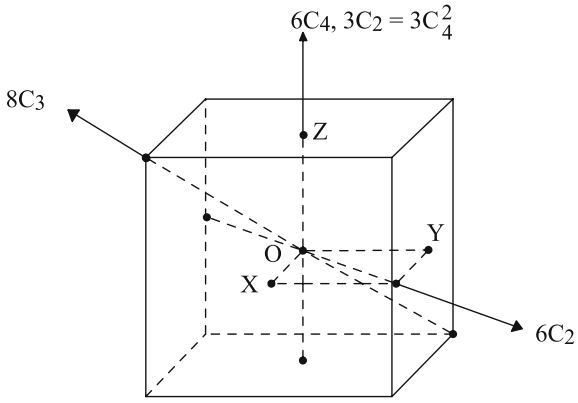

Fig. 12.2. Diagram of cubic symmetry operations

Table 12.2. Characters for the equivalence representation $\Gamma^{\text{equiv.}}$ for the five lowest energy levels of plane wave states labeled by $\{\boldsymbol{K}_{n_i}\}$ using the notation of Table 12.1

$\boldsymbol{K}_{n_i}$	E	$3C_4^2$	$6C_2$	$8C_3$	$6C_4$	i	$3iC_4^2$	$6iC_2$	$8iC_3$	$6iC_4$	
{0,0,0}	1	1	1	1	1	1	1	1	1	1	Γ_1
{1,0,0}	6	2	0	0	2	0	4	2	0	0	$\Gamma_1 + \Gamma_{12} + \Gamma_{15}$
{1,1,0}	12	0	2	0	0	0	4	2	0	0	$\Gamma_1 + \Gamma_{12} + \Gamma_{15} + \Gamma_{25'} + \Gamma_{25}$
{1,1,1}	8	0	0	2	0	0	0	4	0	0	$\Gamma_1 + \Gamma_2 + \Gamma_{15} + \Gamma_{25'}$
{2,0,0}	6	2	0	0	2	0	4	2	0	0	$\Gamma_1 + \Gamma_{12} + \Gamma_{15}$

The irreducible representations for each energy level contained in $\Gamma^{\text{equiv.}}$ are listed in the right-hand column

the symmetry operations of O_h, a contribution of one is made to the character; otherwise a zero contribution is made. Using these definitions, we obtain the characters $\chi^{\text{equiv.}}$ and the characters for the various plane waves are given in Table 12.2, where the various plane wave states are denoted by one of the reciprocal lattice vectors which describe each of these states using the notation of Table 12.1. The reducible representations $\Gamma^{\text{equiv.}}$ for the various plane wave states in the simple cubic lattice are decomposed into irreducible representations of O_h and the results are given on the right-hand side of Table 12.2.

Once we know the irreducible representations of O_h that are contained in each of the degenerate levels of the simple cubic empty lattice, we can find appropriate linear combinations of these plane wave states which will then transform as the desired irreducible representations of O_h. When a cubic periodic potential is now applied, the degeneracy of these empty lattice states will be lifted in accordance with the decomposition of the reducible representations of $\Gamma^{\text{equiv.}}$ into the irreducible representations of O_h. Thus the proper linear combinations of the plane wave states will bring the secular equation of the nearly free electron model energy bands into block diagonal form. As an example of how this works, let us list the six appropriate linear combinations for

the $\{1,0,0\}$ set of reciprocal lattice vectors $\exp(\pm 2\pi \mathrm{i} x/a)$, $\exp(\pm 2\pi \mathrm{i} y/a)$, and $\exp(\pm 2\pi \mathrm{i} z/a)$ which will bring the secular equation into block diagonal form:

$$\frac{1}{\sqrt{6}}[(1,0,0)+(\bar{1},0,0)+(0,1,0)+(0,\bar{1},0)+(0,0,1)+(0,0,\bar{1})] \to \Gamma_1$$

$$\left.\begin{aligned} \frac{1}{\sqrt{6}}[(1,0,0)+(\bar{1},0,0)+\omega(0,1,0)+\omega(0,\bar{1},0) \\ +\omega^2(0,0,1)+\omega^2(0,0,\bar{1})] \\ \frac{1}{\sqrt{6}}[(1,0,0)+(\bar{1},0,0)+\omega^2(0,1,0)+\omega^2(0,\bar{1},0) \\ +\omega(0,0,1)+\omega(0,0,\bar{1})] \end{aligned}\right\} \to \Gamma_{12}$$

$$\left.\begin{aligned} \frac{1}{i\sqrt{2}}[(1,0,0)-(\bar{1},0,0)] \\ \frac{1}{i\sqrt{2}}[(0,1,0)-(0,\bar{1},0)] \\ \frac{1}{i\sqrt{2}}[(0,0,1)-(0,0,\bar{1})] \end{aligned}\right\} \to \Gamma_{15}\,, \tag{12.13}$$

in which we have used (1,0,0) to denote $\exp(2\pi \mathrm{i} x/a)$ and correspondingly for the other plane waves. Here $\omega = 2\pi \mathrm{i}/3$ and we note that Γ_1 and Γ_{12} are even under inversion, but Γ_{15} is odd under inversion. Substituting

$$\begin{aligned} \frac{1}{2}[(1,0,0)+(\bar{1},0,0)] &= \cos(2\pi x/a) \\ \frac{1}{2i}[(1,0,0)-(\bar{1},0,0)] &= \sin(2\pi x/a)\,, \end{aligned} \tag{12.14}$$

we obtain the following linear combinations of symmetrized plane waves from (12.13):

$$\frac{2}{\sqrt{6}}\left[\cos\left(\frac{2\pi x}{a}\right)+\cos\left(\frac{2\pi y}{a}\right)+\cos\left(\frac{2\pi z}{a}\right)\right] \to \Gamma_1$$

$$\left.\begin{aligned} \frac{2}{\sqrt{6}}\left[\cos\left(\frac{2\pi x}{a}\right)+\omega\cos\left(\frac{2\pi y}{a}\right)+\omega^2\cos\left(\frac{2\pi z}{a}\right)\right] \\ \frac{2}{\sqrt{6}}\left[\cos\left(\frac{2\pi x}{a}\right)+\omega^2\cos\left(\frac{2\pi y}{a}\right)+\omega\cos\left(\frac{2\pi z}{a}\right)\right] \end{aligned}\right\} \to \Gamma_{12}$$

$$\left.\begin{aligned} \sqrt{2}\sin\left(\frac{2\pi x}{a}\right) \\ \sqrt{2}\sin\left(\frac{2\pi y}{a}\right) \\ \sqrt{2}\sin\left(\frac{2\pi z}{a}\right) \end{aligned}\right\} \to \Gamma_{15}\,. \tag{12.15}$$

The linear combinations of plane wave states given in (12.15) transform as irreducible representations of O_h, and bring the secular equation for $E(k=0)$ into block diagonal form. For example, using the six combinations of plane wave states given in (12.15), we bring the (6×6) secular equation for $\boldsymbol{K}_{n_i}=\{1,0,0\}$ into a (1×1), a (2×2) and a (3×3) block, with no coupling between the blocks. Since there are three distinct energy levels, each corresponding to a different symmetry type, the introduction of a weak periodic potential will, in general, split the sixfold level into three levels with degeneracies 1 (Γ_1), 2 (Γ_{12}) and 3 (Γ_{15}). This procedure is used to simplify the evaluation of $E(\boldsymbol{k})$ and $\psi_k(\boldsymbol{r})$ in first-order degenerate perturbation theory. Referring to Table 12.1, (12.15) gives the symmetrized wave functions for the six $K_{\{1,0,0\}}$ vectors. The corresponding analysis can be done for the twelve $K_{\{110\}}$ vectors for the third lowest energy level, etc. The results for $E(\boldsymbol{k})$ for the empty lattice for the simple cubic group #221 are shown in Fig. 12.3 for the $\Gamma-X$ and $\Gamma-R$ axes.

The results obtained for the simple cubic lattice can be extended to other cubic lattices (see Appendix C). The space group numbers for common cubic crystals are as follows: simple cubic (#221), FCC (#225), diamond (#227), BCC (#229) (using standard references such as [54] and [58]). For the FCC lattice the (n_1,n_2,n_3) integers are all even or all odd so that the allowed $\boldsymbol{K}_{n_i}$ vectors are $\{000\}$, $\{1,1,1\}$, $\{200\}$, etc. (see for example: [6] or [45]). For the BCC lattice, the integers $(n_1+n_2+n_3)$ must all sum to an even number, so that we can have reciprocal lattice $\boldsymbol{K}_{n_i}$ vectors $\{000\}$, $\{1,1,0\}$, $\{200\}$, etc. Thus Table 12.1 can be used together with an analysis, such as given in this section, to obtain the proper linear combination of plane waves for the pertinent $\boldsymbol{K}_{n_i}$ vectors for the various cubic groups. These issues are clarified in Problem 12.2. In this problem a weak periodic potential is considered. Then the character tables for the group of the wave vector in Appendix C will be of use.

To complete the discussion of the use of group theory for the solution of the electronic states of the empty lattice (or more generally the nearly free electron) model, we will next consider the construction of the symmetrized plane wave states $E(\boldsymbol{k})$ as we move away from $\boldsymbol{k}=0$.

12.3 Symmetrized Plane Wave Solutions along the Δ-Axis

As an example of a nonzero $\boldsymbol{k}$ vector, let us consider $E(\boldsymbol{k})$ as we move from $\Gamma(\boldsymbol{k}=0)$ toward point $X[\boldsymbol{k}=\pi/a(1,0,0)]$ along the (1,0,0) axis (labeled Δ in Figs. 10.3 and 12.4). The appropriate point group of the wave vector $\boldsymbol{k}$ is C_{4v}, with the character table given in Table 10.3 (see also Table A.16).

In Table 12.3 are listed the characters for the three irreducible representations of $\boldsymbol{K}_{n_i}=\{1,0,0\}(2\pi/a)$ corresponding for the simple cubic empty lattice dispersion relations at $\boldsymbol{k}=0$ and O_h symmetry. We consider these

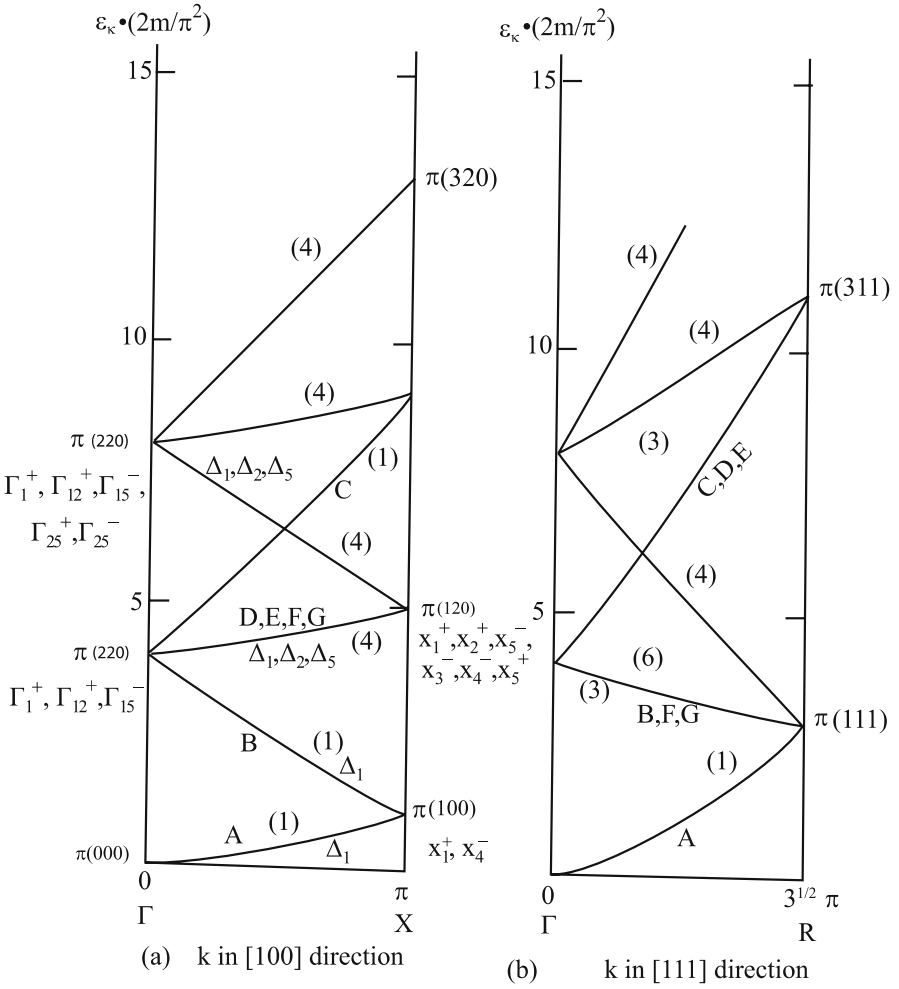

Fig. 12.3. Diagram of the empty lattice energy levels along (**a**) Γ-X and (**b**) Γ-R for the simple cubic lattice #221. See the text for the symmetries of the energy bands that are degenerate at the high symmetry points of the simple cubic empty lattice model

as reducible representations of point group C_{4v}. The decomposition of these three reducible representations in C_{4v} point group symmetry is indicated on the right of Table 12.3. This decomposition yields the compatibility relations (see Sect. 10.7):

$$\begin{aligned} \Gamma_1 &\to \Delta_1 \\ \Gamma_{12} &\to \Delta_1 + \Delta_2 \\ \Gamma_{15} &\to \Delta_1 + \Delta_5 \,. \end{aligned} \tag{12.16}$$

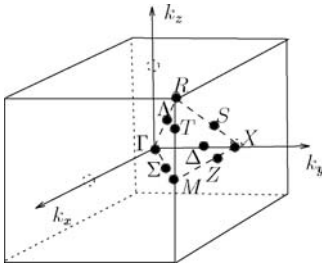

Fig. 12.4. Brillouin zone for a simple cubic lattice showing high symmetry points

Table 12.3. Characters for the three symmetrized plane waves (12.16) corresponding to the six plane waves $\boldsymbol{K}_{n_i} = (2\pi/a)(1,0,0)$ in Table 12.1[a,b]

C_{4v} $(4mm)$	E	C_2	$2C_4$	$2\sigma_v$	$2\sigma_d$	
Γ_1	1	1	1	1	1	Δ_1
Γ_{12}	2	2	0	2	0	$\Delta_1+\Delta_2$
Γ_{15}	3	−1	1	1	1	$\Delta_1+\Delta_5$

[a] The characters for each symmetrized plane wave at $k = 0$ with O_h symmetry is considered as a reducible representation in the $C_{4v}(4mm)$ group which is appropriate for the wave vector $\boldsymbol{k}$ along a cubic axis. The decomposition of the reducible representations into their irreducible components along the Δ axis are indicated using the notation of the character table for C_{4v}

[b] The operation σ_v denotes iC_2^{010} and iC_2^{001}, while σ_d denotes iC_2^{011} and $iC_2^{01\bar{1}}$

In the character table (Table 12.3), the main symmetry axis is the x-axis, so that the basis functions that should be used (see Table A.16) require the transformation: $x \to y$, $y \to z$, $z \to x$. The symmetry axis $\sigma_v = iC_2^{010}$ denotes the mirror planes $y = 0$ and $z = 0$, while $\sigma_d = iC_2^{011}$ denotes the diagonal (011) planes, with all symmetry operations referring to reciprocal space, since we are considering the group of the wave vector at a point along the Δ axis. The results of (12.16) are of course in agreement with the compatibility relations given in Sect. 10.7 for the simple cubic structure. Compatibility relations of this type can be used to obtain the degeneracies and symmetries for all the levels at the Δ point, starting from the plane wave solution at $\boldsymbol{k} = 0$. A similar approach can be used to obtain the symmetries and degeneracies as we move away from $\boldsymbol{k} = 0$ in other directions. For an arbitrary crystal structure we have to use standard references or websites [54] to construct the compatibility relations using the tables for the group of the wave vector given in this reference. Some illustrative examples are given in Appendix C.

12.4 Plane Wave Solutions at the *X* Point

As we move in the Brillouin zone from a point of high symmetry to a point of lower symmetry, the solution using the compatibility relations discussed

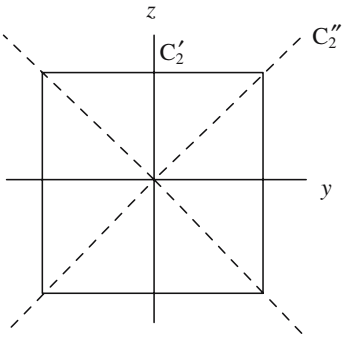

Fig. 12.5. Diagram of a square showing the twofold axes normal to the principal C_4 symmetry axis which are pertinent to point group D_{4h}

in Sect. 12.3 is unique. On the other hand, when going from a point of lower symmetry like a Δ point to one of higher symmetry, the solution from the compatibility relations is not unique, and we must then go back to consideration of the equivalence transformation. An example of this situation occurs when we go from the Δ point (see Table C.8) to the X-point (D_{4h} symmetry and Table C.15), which has higher symmetry than the Δ point (C_{4v} symmetry). The appropriate character table for the group of the wave vector at the X point (see Table C.15 in Appendix C) is $D_{4h} = D_4 \otimes i$ shown in Table A.18. At the X-point, the nearly free electron solutions for the simple cubic lattice given by (12.7) become:

$$E\left(\boldsymbol{k} = \frac{\pi}{a}\hat{x}\right) = \frac{\hbar^2}{2m}\left(\frac{2\pi}{a}\right)^2\left[\left(\frac{1}{2} + n_1\right)^2 + n_2^2 + n_3^2\right] . \tag{12.17}$$

The lowest energy level at the X-point is

$$E_1\left(\boldsymbol{k} = \frac{\pi}{a}\hat{x}\right) = \frac{\hbar^2}{2m}\left(\frac{2\pi}{a}\right)^2\left(\frac{1}{4}\right) . \tag{12.18}$$

The pertinent plane waves which contribute to the energy level E_1 in (12.18) correspond to $\boldsymbol{K}_{n_i}$ vectors

$$\boldsymbol{K}_{n_i} = (0,0,0)$$
$$\boldsymbol{K}_{n_i} = \frac{2\pi}{a}(\bar{1},0,0) .$$

We will now find $\chi^{\text{equiv.}}$ for these plane waves, using the symmetry operations in Fig. 12.5 and in the character table for D_{4h} in which we use the transformation $x \to y$, $y \to z$, $z \to x$ to obtain the proper X-point (Table 12.4). We note that the plane wave labeled $\boldsymbol{K}_{n_i} = (0,0,0)$ in Table 12.1 yields a plane wave $\mathrm{e}^{(\pi i/a)x}$ at the X-point while the plane wave labeled

Table 12.4. Character table for the point group D_4, showing the solid state notation in the right-hand column

D_4 (422)			E	$C_2 = C_4^2$	$2C_4$	$2C_2'$	$2C_2''$	
$x^2 + y^2, z^2$		A_1	1	1	1	1	1	X_1
	R_z, z	A_2	1	1	1	-1	-1	X_4
$x^2 - y^2$		B_1	1	1	-1	1	-1	X_2
xy		B_2	1	1	-1	-1	1	X_3
(xz, yz)	(x, y) (R_x, R_y)	E	2	-2	0	0	0	X_5

With inversion $D_{4h} = D_4 \otimes i$

Table 12.5. Characters for the two plane waves with energy E_1 for the simple cubic empty lattice electron dispersion relations at the X point (D_{4h} symmetry)

	E	C_2	$2C_4$	$2C_2'$	$2C_2''$	i	iC_2	$2iC_4$	$2iC_2'$	$2iC_2''$	
$\exp(\pm\pi i x/a)$	2	2	2	0	0	0	0	0	2	2	$A_{1g} + A_{2u}$

$\boldsymbol{K}_{n_i} = (2\pi/a)(\bar{1}, 0, 0)$ in Table 12.1 yields a plane wave $\mathrm{e}^{\left(\frac{\pi}{a} ix - \frac{2\pi}{a} ix\right)} = \mathrm{e}^{-\frac{\pi}{a} ix}$ and both have energies $E_1 = \hbar^2/2m \left(\frac{2\pi}{a}\right)^2 (1/4)$. The plane waves denoted by $\boldsymbol{K}_{n_i} = (0, 0, 0)$ and $\boldsymbol{K}_{n_i} = 2\pi/a(\bar{1}, 0, 0)$ form partners of a reducible representation, and the characters for these two plane waves in the equivalence transformation $\Gamma^{\text{equiv.}}$ are here shown to yield (Table 12.5):

$$\Gamma^{\text{equiv.}} = X_1^+ + X_4^- \,. \tag{12.19}$$

We thus obtain irreducible representations with X_1^+ and X_4^- symmetries for the lowest X-point level so that a periodic potential will split the degeneracy of these levels at the X-point. In this case the level separation becomes $2|V_{\boldsymbol{K}_{n_i}}|$ (see for example [6, 45]) where $\boldsymbol{K}_{n_i} = (2\pi/a)(\bar{1}, 0, 0)$. The appropriate linear combination of plane waves corresponding to the X_1^+ and X_4^- irreducible representations are

$$\begin{aligned} X_1^+ \text{ symmetry:} \quad & (0,0,0) + (\bar{1},0,0) \rightarrow 2\cos\frac{\pi}{a}x \\ X_4^- \text{ symmetry:} \quad & (0,0,0) - (\bar{1},0,0) \rightarrow 2\sin\frac{\pi}{a}x \,. \end{aligned} \tag{12.20}$$

and each of the X_1^+ and X_4^- levels is nondegenerate. Referring to (12.17), the next lowest energy level at the X point is

$$E_2\left(\boldsymbol{k} = \frac{\pi}{a}\hat{x}\right) = \frac{\hbar^2}{2m}\left(\frac{2\pi}{a}\right)^2\left(\frac{5}{4}\right) . \tag{12.21}$$

Table 12.6. Characters for the plane waves comprising state with energy E_2 at the X point (D_{4h} symmetry) for the simple cubic empty lattice electronic energy bands

	E	C_2	$2C_4$	$2C_2'$	$2C_2'$	i	iC_2	$2iC_4$	$2iC_2'$	$2iC_2''$
(12.22)	8	0	0	0	0	0	0	0	4	0
$\exp(\pm 2\pi i y/a)$	4	0	0	2	0	0	4	0	2	0
$\exp(\pm 2\pi i z/a)$										

The eight pertinent plane waves for this energy level correspond to the $\boldsymbol{K}_{n_i}$ vectors

$$\boldsymbol{K}_{n_i} = \frac{2\pi}{a}(0,1,0), \frac{2\pi}{a}(0,\bar{1},0), \frac{2\pi}{a}(0,0,1), \frac{2\pi}{a}(0,0,\bar{1})$$
$$\boldsymbol{K}_{n_i} = \frac{2\pi}{a}(\bar{1},1,0), \frac{2\pi}{a}(\bar{1},\bar{1},0), \frac{2\pi}{a}(\bar{1},0,1), \frac{2\pi}{a}(\bar{1},0,\bar{1})$$

in Table 12.1. More explicitly, the eight plane waves corresponding to these $\boldsymbol{K}_{n_i}$ vectors are

$$\exp\left\{\frac{\pi i x}{a} + \frac{2\pi i y}{a}\right\}, \ \exp\left\{\frac{\pi i x}{a} - \frac{2\pi i y}{a}\right\},$$
$$\exp\left\{\frac{\pi i x}{a} + \frac{2\pi i z}{a}\right\}, \ \exp\left\{\frac{\pi i x}{a} - \frac{2\pi i z}{a}\right\},$$
$$\exp\left\{\frac{-\pi i x}{a} + \frac{2\pi i y}{a}\right\}, \ \exp\left\{-\frac{\pi i x}{a} - \frac{2\pi i y}{a}\right\},$$
$$\exp\left\{-\frac{\pi i x}{a} + \frac{2\pi i z}{a}\right\}, \ \exp\left\{-\frac{\pi i x}{a} - \frac{2\pi i z}{a}\right\}. \qquad (12.22)$$

To find the characters for the equivalence transformation for the eight plane waves of (12.22) we use the character table for D_{4h} and Fig. 12.5. The results for several pertinent plane wave combinations are given in Table 12.6. The reducible representation for the eight plane waves given by (12.22) yields the following X-point irreducible representations

$$X_1^+ + X_2^+ + X_5^- + X_4^- + X_3^- + X_5^+ . \qquad (12.23)$$

The same result can be obtained by considering the $e^{\pm \pi i x/a}$ functions as common factors of the $e^{\pm 2\pi i y/a}$ and $e^{\pm 2\pi i z/a}$ functions. The $\chi^{\text{equiv.}}$ for the four $e^{\pm 2\pi i y/a}$ and $e^{\pm 2\pi i z/a}$ plane waves is also tabulated in Table 12.6. The $e^{\pm \pi i x/a}$ functions transform as $X_1^+ + X_4^-$ (see (12.19)), and the four functions $e^{\pm 2\pi i y/a}$ and $e^{\pm 2\pi i z/a}$ transform as $X_1^+ + X_2^+ + X_5^-$. If we now take the direct product indicated in (12.24), we obtain

$$(X_1^+ + X_4^-) \otimes (X_1^+ + X_2^+ + X_5^-) = X_1^+ + X_2^+ + X_5^- + X_4^- + X_3^- + X_5^+ \quad (12.24)$$

in agreement with the result of (12.23). The proper linear combination of the eight plane waves which transform as irreducible representations of the D_{4h} point symmetry group for the second lowest X point level is found from the $\boldsymbol{K}_{n_i}$ vectors given in (16.16):

$$
\begin{aligned}
X_1^+ :\ & (0,1,0)+(0,\bar{1},0)+(0,0,1)+(0,0,\bar{1}) \\
& +(\bar{1},1,0)+(\bar{1},\bar{1},0)+(\bar{1},0,1)+(\bar{1},0,1) \\
X_4^- :\ & (0,1,0)+(0,\bar{1},0)+(0,0,1)+(0,0,\bar{1}) \\
& -(\bar{1},1,0)-(\bar{1},\bar{1},0)-(\bar{1},0,1)-(\bar{1},0,1) \\
X_2^+ :\ & (0,1,0)-(0,0,1)+(0,\bar{1},0)-(0,0,\bar{1}) \\
& +(\bar{1},1,0)-(\bar{1},0,1)+(\bar{1},\bar{1},0)-(\bar{1},0,\bar{1}) \\
X_3^- :\ & (0,1,0)-(0,0,1)+(0,\bar{1},0)-(0,0,\bar{1}) \\
& -(\bar{1},1,0)+(\bar{1},0,1)-(\bar{1},\bar{1},0)+(\bar{1},0,\bar{1}) \\
X_5^- :\ & \left.\begin{matrix}(0,1,0)-(0,\bar{1},0)+(\bar{1},1,0)-(\bar{1},\bar{1},0) \\ (0,0,1)-(0,0,\bar{1})+(\bar{1},0,1)-(\bar{1},0,\bar{1})\end{matrix}\right\} \text{two partners} \\
X_5^+ :\ & \left.\begin{matrix}(0,1,0)-(0,\bar{1},0)-(\bar{1},1,0)+(\bar{1},\bar{1},0) \\ (0,0,1)-(0,0,\bar{1})-(\bar{1},0,1)+(\bar{1},0,\bar{1})\end{matrix}\right\} \text{two partners}\,, \qquad (12.25)
\end{aligned}
$$

in which the plane waves are denoted by their corresponding $\boldsymbol{K}_{n_i}$ vectors. We note that the wave vector $\boldsymbol{K}_{n_i} = (2\pi/a)(0,1,0)$ gives rise to a plane wave $\exp[(\pi ix/a)+(2\pi iy/a)]$. Likewise the wave vector $\boldsymbol{K}_{n_i} = (2\pi/a)(\bar{1},1,0)$ gives rise to a plane wave $\exp[(\pi ix/a)-(2\pi ix/a)+(\pi iy/a)]$. Using this notation we find that the appropriate combinations of plane waves corresponding to (12.25) are

$$
\begin{aligned}
X_1^+ :\ & \cos\frac{\pi x}{a}\left(\cos\frac{2\pi y}{a}+\cos\frac{2\pi z}{a}\right) \\
X_4^- :\ & \sin\frac{\pi x}{a}\left(\cos\frac{2\pi y}{a}+\cos\frac{2\pi z}{a}\right) \\
X_2^+ :\ & \cos\frac{\pi x}{a}\left(\cos\frac{2\pi y}{a}-\cos\frac{2\pi z}{a}\right) \\
X_3^- :\ & \sin\frac{\pi x}{a}\left(\cos\frac{2\pi y}{a}-\cos\frac{2\pi z}{a}\right) \\
X_5^- :\ & \left.\begin{matrix}\cos\dfrac{\pi x}{a}\sin\dfrac{2\pi y}{a} \\ \cos\dfrac{\pi x}{a}\sin\dfrac{2\pi z}{a}\end{matrix}\right\} \text{two partners} \\
X_5^+ :\ & \left.\begin{matrix}\sin\dfrac{\pi x}{a}\sin\dfrac{2\pi y}{a} \\ \sin\dfrac{\pi x}{a}\sin\dfrac{2\pi z}{a}\end{matrix}\right\} \text{two partners}\,. \qquad (12.26)
\end{aligned}
$$

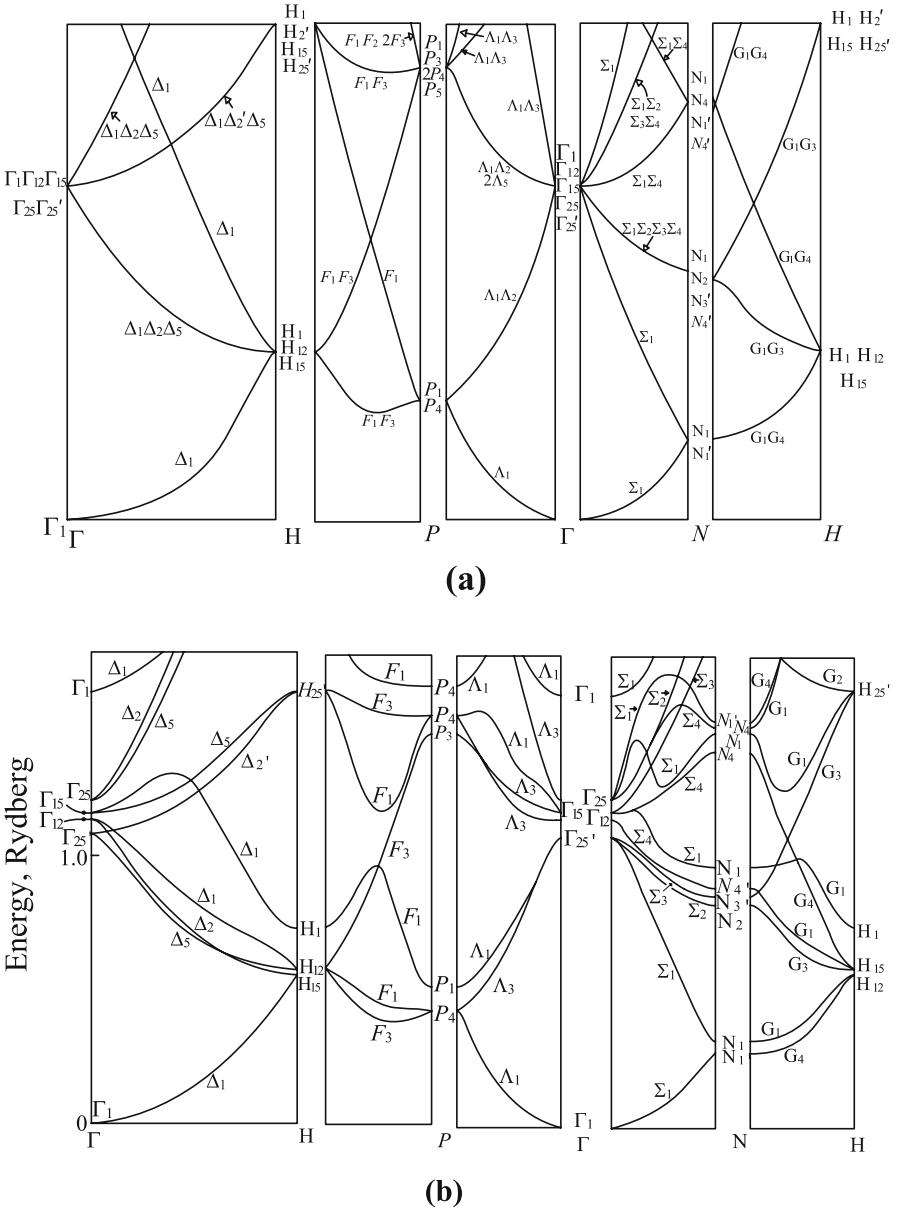

Fig. 12.6. (**a**) $E(\boldsymbol{k})$ for a BCC lattice in the empty lattice approximation, $V \equiv 0$. (**b**) $E(\boldsymbol{k})$ for sodium, showing the effect of a weak periodic potential in lifting accidental band degeneracies at $k = 0$ and at the zone boundaries (high symmetry points) in the Brillouin zone. Note that the splittings are quite different for the various bands and at different high symmetry points. The character tables in Appendix C for the group of the wave vector for the BCC lattice are useful for solving the problem of the electronic structure for a nearly free electron model for a BCC alkali metal

A summary of the energy levels and symmetries along $\Gamma - X$ for the simple cubic lattice is given in Fig. 12.3(a). A similar procedure is used to find the degeneracies and the symmetrized linear combination of plane waves for any of the energy levels at each of the high symmetry points in the Brillouin zone. We show for example results in Fig. 12.3(b) also for the empty lattice bands along $\Gamma - R$. The corresponding results can be obtained by this same procedure for the FCC and BCC lattices as well (see Figs. 12.1 and 12.6). Some elaboration of these concepts is found in Problems 12.2 and 12.6.

In the following section we will consider the effect of nonsymmorphic operations on plane waves.

12.5 Effect of Glide Planes and Screw Axes

Up to this point we have considered only symmorphic space groups where the symmetry operations of the group of the wave vectors are simply point group operations. The main effect of the glide planes and screw axes in nonsymmorphic space groups on the group of the wave vector is to cause energy bands to stick together along some of the high symmetry points and axes in the Brillouin zone. We first illustrate this phenomenon using the 2D space group $p2mg$ (#7) which has a twofold axis, mirror planes normal to the x-axis at $x = 1/4a$ and $x = 3/4a$, and a glide plane g parallel to the x-axis with a translation distance $a/2$. In addition, group $p2mg$ has inversion symmetry. Suppose that $X(x, y)$ is a solution to Schrödinger's equation at the X point $\boldsymbol{k}_X = \pi/a(1, 0)$ (see Fig. 12.7).

In the two-dimensional case for the space group $p2mg$, the mirror glide operation g implies

$$gX(x, y) = X\left(x + \frac{1}{2}a, -y\right) , \tag{12.27}$$

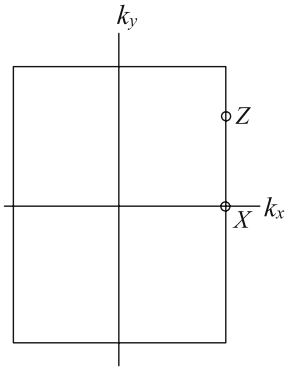

Fig. 12.7. Brillouin zone for a rectangular 2D lattice [such as $p2mg$ (#7)]

while inversion i implies

$$iX(x,y) = X(-x,-y)\,. \tag{12.28}$$

The mirror plane m at $x = a/4$ implies

$$mX(x,y) = X\left(-x + \frac{1}{2}a, y\right)\,, \tag{12.29}$$

so that

$$gX(x,y) = m\; iX(x,y)\,, \tag{12.30}$$

where m denotes reflection in a mirror plane and i denotes inversion. Since $i^2X(x,y) = X(x,y)$ and $m^2X(x,y) = X(x,y)$, we would expect from (12.30) that

$$g^2X(x,y) = X(x,y)\,. \tag{12.31}$$

But direct application of the glide operation twice yields for $k_x = \pi/a$,

$$g^2X(x,y) = X(x+a,y) = \mathrm{e}^{ik_x a}X(x,y) = \mathrm{e}^{\pi i}X(x,y) = -X(x,y)\,, \tag{12.32}$$

which contradicts (12.31). This contradiction is resolved by having the solutions that $\pm X(x,y)$ stick together at the X point.

In fact, if we employ time reversal symmetry (to be discussed in Chap. 16), we can show that bands $\pm\Phi_Z(x,y)$ stick together along the entire Brillouin zone edge for all Z points, i.e., $(\pi/a, k_y)$ (see Fig. 12.7). Thus in addition to the degeneracies imposed by the group of the wave vector, other symmetry relations can in some cases cause energy bands to stick together at high symmetry points and axes.

The same situation also arises for 3D space groups. Some common examples where energy bands stick together are on the hexagonal face of the hexagonal close-packed structure (space group #194, see Brillouin zone in Fig. 12.8(a)), and the square face in the diamond structure (#227) for which the Brillouin zone is given in Fig. 12.8(b). For the case of the hexagonal close packed structure, there is only a single translation $\boldsymbol{\tau} = (c/2)(0,0,1)$ connected with nonsymmorphic operations in space group #194. The character table for the group of the wave vector at the A point (see Table C.26) shows that the bands stick together, i.e., there are no nondegenerate levels at the A point. To illustrate this point, we give in Tables C.24 and C.26 the character tables for the Γ point and the A point, respectively, for space group #194.

For the case of the diamond structure (space group #227), Miller and Love [54] show that there are three different translation vectors $(a/4)(1,1,0)$, $(a/4)(0,1,1)$, and $(a/4)(1,0,1)$ can be used to describe the nonsymmorphic aspects of the diamond structure [54]. The reason why these translations differ from those used in this section (see Fig. 10.6) is the selection of a different origin for the unit cell. In Miller and Love [54] the origin is selected to lie

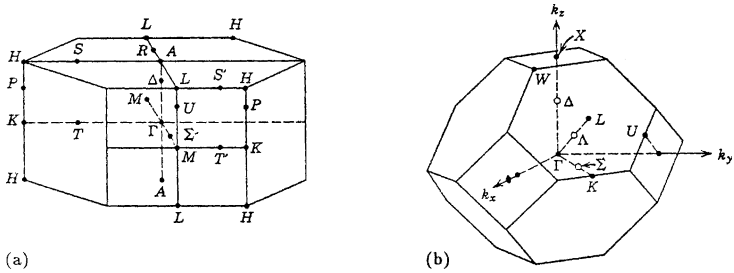

Fig. 12.8. Brillouin zone for (**a**) the hexagonal close packed structure, D^4_{6h}, #194 and (**b**) the FCC structure (e.g., diamond #227) in which the high symmetry axes are emphasized (see also Fig. C.5).

halfway between the two inequivalent lattice points, which is at $a/8(1,1,1)$ or at $a/8(\bar{1},\bar{1},\bar{1})$, so that the inversion operation takes the white sublattice into a black sublattice, and vice versa. In contrast, we have taken the origin in Sect. 10.8 to coincide with the origin of the white sublattice so that in this case the space group operation for inversion contains a translation by $\boldsymbol{\tau} = (a/4)(1,1,1)$ and is denoted by $\{i|\tau\}$.

In Table C.17, we show the character tables for the group of the wave vector appropriate for the diamond structure at the Γ point. The behavior of $E(\boldsymbol{k})$ at $\boldsymbol{k} = 0$ for the diamond structure is similar to that for a symmorphic cubic like the FCC structure. Furthermore, at the L-point in the Brillouin zone, the structure factor does not vanish:

$$\sum_j \mathrm{e}^{i\boldsymbol{K}_{n_L}\cdot\boldsymbol{r}_j} = 1 + \mathrm{e}^{i2\pi/a(1,1,1)\cdot a/4(1,1,1)} = 1 - i \neq 0\,, \tag{12.33}$$

and the behavior of $E(\boldsymbol{k})$ is expected to be similar to the behavior of a symmorphic cubic space group like that for the FCC structure, space group #225. Thus for the nonsymmorphic diamond structure, some high symmetry points behave normally (such as the L point), while for other points (such as the X point as we discuss below), the energy bands stick together.

Next we show that the nonsymmorphic nature of the diamond structure strongly affects the empty lattice energy band structure and is totally an effect of symmetry considerations. Application of the empty lattice plane wave energies for the first few lowest energy states at $k = 0$ (Γ point), the L-point, and the X-point are shown in Table 12.7, and the corresponding empty lattice $E(\boldsymbol{k})$ diagram is shown in Fig. 12.9. The twofold, fourfold and eightfold degenerate levels at the X-point are noted with the empty lattice nondegenerate bands coming into the X-point with equal and opposite slopes.

At the X point (Table 10.12) we see that there are no nondegenerate levels so that levels stick together (see Sect. 10.8). In the $E(\boldsymbol{k})$ diagram for the diamond structure (see Fig. 12.10 for $E(\boldsymbol{k})$ for Ge), we see that all the bands stick together at the X point, all being either twofold or fourfold degenerate,

Table 12.7. Classification of the empty lattice eigenvalues at the symmetry points Γ, L and X of the diamond structure (#227)

	number of plane waves	empty lattice eigenvalues in units of $(\hbar^2/2m)(4\pi^2/a^2)$	irreducible representations
point Γ	1	(0,0,0)	Γ_1
$\boldsymbol{k} = (0,0,0)$	8	(1,1,1)	$\Gamma_1 \quad \Gamma'_{25} \quad \Gamma_{15} \quad \Gamma'_2$
	6	(2,0,0)	$\Gamma'_{25} \quad \Gamma'_{12} \quad \Gamma'_2$
	12	(2,2,0)	$\Gamma_1 \quad \Gamma'_{25} \quad \Gamma_{15} \quad \Gamma_{12} \quad \Gamma_{25}$
point L	2	$\left(\frac{1}{2},\frac{1}{2},\frac{1}{2}\right)$	$L_1 \quad L'_2$
$\boldsymbol{k} = \frac{2\pi}{a}\left(\frac{1}{2},\frac{1}{2},\frac{1}{2}\right)$	6	$\left(\frac{3}{2},\frac{1}{2},\frac{1}{2}\right)$	$L_1 \quad L'_2 \quad L_3 \quad L'_3$
	6	$\left(\frac{1}{2},\frac{3}{2},\frac{3}{2}\right)$	$L_1 \quad L'_2 \quad L_3 \quad L'_3$
	6	$\left(\frac{5}{2},\frac{1}{2},\frac{1}{2}\right)$	$L_1 \quad L'_2 \quad L_3 \quad L'_3$
	2	$\left(\frac{3}{2},\frac{3}{2},\frac{3}{2}\right)$	$L_1 \quad L'_2$
point X	2	(1,0,0)	X_1
$\boldsymbol{k} = \frac{2\pi}{a}(1,0,0)$	4	(0,1,1)	$X_1 \quad X_4$
	8	(1,2,0)	$X_1 \quad X_2 \quad X_3 \quad X_4$
	8	(2,1,1)	$2X_1 \quad X_3 \quad X_4$

as seen in the character table for the X point in Table 10.12 and in the empty lattice model in Table 12.7. The plane wave basis functions for the irreducible representations X_1, X_2, X_3 and X_4 for the diamond structure are listed in Table 12.8 and are consistent with these symmetry requirements.

Because of the nonsymmorphic features of the diamond structure, the energy bands at the X point behave differently from the bands at high symmetry points where "essential" degeneracies occur. For the case of essential degeneracies, the energy bands $E(\boldsymbol{k})$ come into the Brillouin zone with zero slope. For the X point in the diamond structure, the $E(\boldsymbol{k})$ dispersion relations with X_1 and X_2 symmetry in general have a nonzero slope, but rather the slopes are equal and opposite for the two levels X_1 and X_2 that stick together. The physical reason for this behavior is that the X-ray structure factor for the Bragg reflection associated with the X point in the Brillouin zone for the diamond structure vanishes and thus no energy discontinuity in $E(\boldsymbol{k})$ is expected, nor is it observed upon small variation of k_x relative to the X point. Explicitly the structure factor [45] at the X point for the diamond structure is

$$\sum_j \mathrm{e}^{i\boldsymbol{K}_{n_X}\cdot\boldsymbol{r}_j} = 1 + \mathrm{e}^{i4\pi/a(1,0,0)\cdot a/4(1,1,1)} = 1 - 1 \equiv 0\,, \tag{12.34}$$

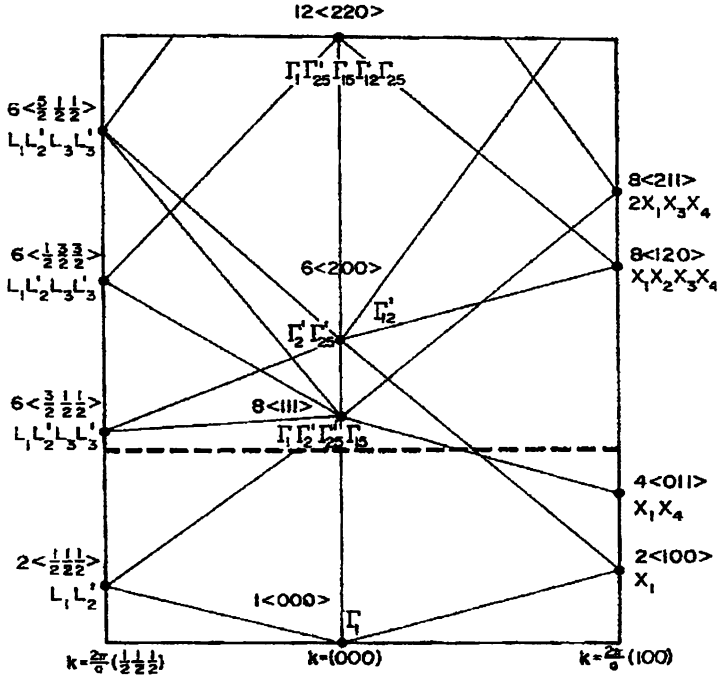

Fig. 12.9. Schematic diagram which indicates the symmetry types of the empty lattice energy levels along $\Gamma - L$ and $\Gamma - X$ for the diamond structure, space group #227 [10] The *dashed horizontal line* indicates the Fermi level on the empty lattice model for four electrons per atom, indicating that the empty lattice model gives a semimetal for the diamond structure for group IV materials. We therefore conclude that the empty lattice model is not a good approximation for semiconductors crystallizing in the diamond structure

where $K_{n_X} = (2\pi/a)(1,0,0)$ for the FCC structure from Table 12.1 and the sum is over the two inequivalent atom sites in the unit cell [one is at the origin and the other is at $(a/4)(1,1,1)$]. The vanishing of this structure factor for the reciprocal lattice vector $\boldsymbol{K}_{n_X} = (4\pi/a)(1,0,0)$ associated with the X point implies that there is no Fourier component of the periodic potential to split the degeneracy caused by having two atoms of the same chemical species per unit cell and thus the energy bands at the X-point stick together. In fact, the structure factor in the diamond structure vanishes for all points on the square face of the FCC Brillouin zone (see Fig. 12.8(b)), and we have energy bands sticking together across the entire square face. A comparison between the empty lattice energy band symmetries for the X-point of the FCC lattice (Fig. 12.1) and for the diamond structure (Fig. 12.9) highlights the effect of the nonsymmorphic symmetry on the electronic structure near the X-point but not near the L-point.

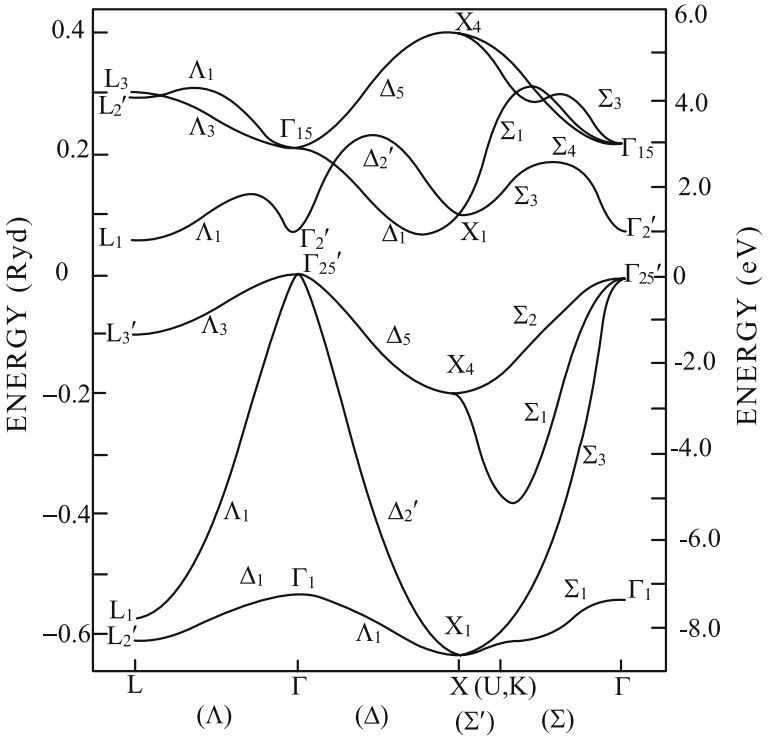

Fig. 12.10. Energy band structure for germanium as an example of a material which is described by a nonsymmorphic space group #227 for the diamond structure. Note that the energy bands stick together at the X point as predicted by group theory (see text). In this diagram the spin-orbit interaction is neglected (see the treatment of double groups in Chap. 14)

To get further insight into how the energy bands at the X-point stick together, consider the operations of the inversion symmetry operator $\{i|\boldsymbol{\tau}_d\}$ on the basis functions for the X-point listed in Table 12.8. To treat the effect of $\{i|\tau_d\}$ on the various functions of (x, y, z) in Table 12.8, consider first the action of $\{i|\boldsymbol{\tau}_d\}$ on the coordinates:

$$\{i|\boldsymbol{\tau}_d\}\begin{pmatrix} x \\ y \\ z \end{pmatrix} = \begin{pmatrix} -x + (a/4) \\ -y + (a/4) \\ -z + (a/4) \end{pmatrix} . \tag{12.35}$$

Then using the trigonometric identity:

$$\begin{aligned} \cos(\alpha + \beta) &= \cos\alpha\cos\beta - \sin\alpha\sin\beta \\ \sin(\alpha + \beta) &= \sin\alpha\cos\beta + \cos\alpha\sin\beta\,, \end{aligned} \tag{12.36}$$

Table 12.8. Plane wave basis functions for the group of the wave vector for the X-point $[2\pi/a(1,0,0)]$ for the nonsymmorphic diamond structure

representation	function
X_1	$x_{11} = \cos\frac{2\pi}{a}x$
	$x_{12} = \sin\frac{2\pi}{a}x$
X_2	$x_{21} = \cos\frac{2\pi}{a}x\left[\cos\frac{4\pi}{a}y - \cos\frac{4\pi}{a}z\right]$
	$x_{22} = \sin\frac{2\pi}{a}x\left[\cos\frac{4\pi}{a}y - \cos\frac{4\pi}{a}z\right]$
X_3	$x_{31} = \sin\frac{4\pi}{a}(y+z)\left[\cos\frac{2\pi}{a}x + \sin\frac{2\pi}{a}x\right]$
	$x_{32} = \sin\frac{4\pi}{a}(y-z)\left[\cos\frac{2\pi}{a}x - \sin\frac{2\pi}{a}x\right]$
X_4	$x_{41} = \sin\frac{4\pi}{a}(y-z)\left[\cos\frac{2\pi}{a}x + \sin\frac{2\pi}{a}x\right]$
	$x_{42} = \sin\frac{4\pi}{a}(y+z)\left[\cos\frac{2\pi}{a}x - \sin\frac{2\pi}{a}x\right]$

we obtain for the effect of $\{i|\boldsymbol{\tau}_d\}$ on the various trigonometric functions in Table 12.8:

$$\begin{aligned}
\{i|\boldsymbol{\tau}_d\}\cos\left(\frac{2\pi}{a}x\right) &= \cos\left(\frac{2\pi}{a}(-x)+\frac{\pi}{2}\right) = \sin\left(\frac{2\pi}{a}x\right)\\
\{i|\boldsymbol{\tau}_d\}\sin\left(\frac{2\pi}{a}x\right) &= \sin\left(\frac{2\pi}{a}(-x)+\frac{\pi}{2}\right) = \cos\left(\frac{2\pi}{a}x\right)\\
\{i|\boldsymbol{\tau}_d\}\cos\left(\frac{4\pi}{a}y\right) &= \cos\left(\frac{4\pi}{a}(-y)+\pi\right) = -\cos\left(\frac{4\pi}{a}y\right)\\
\{i|\boldsymbol{\tau}_d\}\sin\left(\frac{4\pi}{a}y\right) &= \sin\left(\frac{4\pi}{a}(-y)+\pi\right) = \sin\left(\frac{4\pi}{a}y\right)\\
\{i|\boldsymbol{\tau}_d\}\sin\left(\frac{4\pi}{a}(y+z)\right) &= \sin\left(\frac{4\pi}{a}(-y-z)+2\pi\right) = -\sin\left(\frac{4\pi}{a}(y+z)\right)\\
\{i|\boldsymbol{\tau}_d\}\sin\left(\frac{4\pi}{a}(y-z)\right) &= \sin\left(\frac{4\pi}{a}(-y+z)\right) = -\sin\left(\frac{4\pi}{a}(y-z)\right)
\end{aligned} \tag{12.37}$$

Thus we obtain

$$\{i|\boldsymbol{\tau}_d\}\begin{pmatrix}x_{11}\\x_{12}\end{pmatrix} = \begin{pmatrix}\cos\left(\frac{2\pi}{a}(-x)+\frac{\pi}{2}\right)\\ \sin\left(\frac{2\pi}{a}(-x)+\frac{\pi}{2}\right)\end{pmatrix} = \begin{pmatrix}\sin\left(\frac{2\pi}{a}x\right)\\ \cos\left(\frac{2\pi}{a}x\right)\end{pmatrix} = \begin{pmatrix}x_{12}\\x_{11}\end{pmatrix}, \tag{12.38}$$

and we see that the effect of $\{i|\boldsymbol{\tau}_d\}$ is to interchange $x_{11} \leftrightarrow x_{12}$. Similarly the effect of $\{i|\boldsymbol{\tau}_d\}$ on x_{12} and x_{22} is

$$\{i|\boldsymbol{\tau}_d\}\begin{pmatrix} x_{21} \\ x_{22} \end{pmatrix} = \begin{pmatrix} -\sin\left(\frac{2\pi}{a}(x)\right)\left[\cos\left(\frac{4\pi}{a}y\right) - \cos\left(\frac{4\pi}{a}z\right)\right] \\ -\cos\left(\frac{2\pi}{a}(x)\right)\left[\cos\left(\frac{4\pi}{a}y\right) - \cos\left(\frac{4\pi}{a}z\right)\right] \end{pmatrix} = \begin{pmatrix} -x_{22} \\ -x_{21} \end{pmatrix}, \tag{12.39}$$

so that $\{i|\boldsymbol{\tau}_d\}$ in this case interchanges the functions and reverses their signs $x_{21} \leftrightarrow -x_{22}$. Similar results can be obtained by considering other operations that are in the point group O_h (and not in the group T_d), that is by considering symmetry operations involving the translation operation $\boldsymbol{\tau}_d = (a/4)(1,1,1)$. Correspondingly, the other symmetry operations involving translation $\boldsymbol{\tau}_d$ also interchange the basis functions for the X_1 and X_2 irreducible representations.

The physical meaning of this phenomenon is that the energy bands $E_{X_1}(\boldsymbol{k})$ and $E_{X_2}(\boldsymbol{k})$ go right through the X point without interruption in the extended zone scheme, except for an interchange in the symmetry designations of their basis functions in crossing the X point, consistent with the $E(\boldsymbol{k})$ diagram for Ge where bands with X_1 symmetry are seen.

In contrast, the effect of $\{i|\boldsymbol{\tau}_d\}$ on the x_{31} and x_{32} basis functions:

$$\{i|\boldsymbol{\tau}_d\}\begin{pmatrix} x_{31} \\ x_{32} \end{pmatrix} = \begin{pmatrix} -\sin\left(\frac{4\pi}{a}(y+z)\right)\left[\sin\left(\frac{2\pi}{a}x\right) + \cos\left(\frac{2\pi}{a}x\right)\right] \\ -\sin\left(\frac{4\pi}{a}(y-z)\right)\left[\sin\left(\frac{2\pi}{a}x\right) - \cos\left(\frac{2\pi}{a}x\right)\right] \end{pmatrix} = \begin{pmatrix} -x_{31} \\ x_{32} \end{pmatrix} \tag{12.40}$$

does not interchange x_{31} and x_{32}. Thus the X_3 level comes into the X point with zero slope. The behavior for the X_4 levels is similar

$$\{i|\boldsymbol{\tau}_d\}\begin{pmatrix} x_{41} \\ x_{42} \end{pmatrix} = \begin{pmatrix} -\sin\left(\frac{4\pi}{a}(y-z)\right)\left[\sin\left(\frac{2\pi}{a}x\right) + \cos\left(\frac{2\pi}{a}x\right)\right] \\ -\sin\left(\frac{4\pi}{a}(y+z)\right)\left[\sin\left(\frac{2\pi}{a}x\right) - \cos\left(\frac{2\pi}{a}x\right)\right] \end{pmatrix} = \begin{pmatrix} -x_{41} \\ x_{42} \end{pmatrix} \tag{12.41}$$

so that the X_3 and X_4 levels behave like ordinary doubly degenerate levels. Equations (12.38)–(12.41) show that the character $\chi(\{i|\boldsymbol{\tau}_d\})$ vanishes at the X point for the X_1, X_2, X_3 and X_4 levels, consistent with the character table for the diamond X-point given in Table 12.8 (see Problem 12.4). These results also explain the behavior of the energy bands for Ge at the X-point shown in Fig. 12.10. The nondegenerate Δ_1 and $\Delta_{2'}$ energy bands going into the X point stick together and interchange their symmetry designations on crossing the X point, while the doubly degenerate Δ_5 levels go into a doubly-degenerate X_4 level with zero slope at the Brillouin zone boundary. In Chap. 14 we will see that when the spin-orbit interaction is considered the doubly-degenerate X_5 levels are split by the spin–orbit interaction into Δ_6 and Δ_7 levels, and when the spin–orbit interaction is taken into account, all the levels at the X-point have X_5 symmetry and all show sticking-together properties.

Selected Problems

12.1. (a) For the simple cubic lattice find the proper linear combinations of plane waves for the twelve (1,1,0) plane wave states at $\boldsymbol{k} = 0$ which transform as irreducible representations of the O_h point group.
(b) As we move away from $\boldsymbol{k} = 0$, find the plane wave eigenfunctions which transform according to Δ_1 and Δ_5 and are compatible with the eigenfunctions for the Γ_{15}^- level at $k = 0$.
(c) Repeat part (b) for the case of $\Gamma_{12}^+ \rightarrow \Delta_1 + \Delta_2$.

12.2. Using the empty lattice, find the energy eigenvalues, degeneracies and symmetry types for the two electronic levels of lowest energy for the FCC lattice at the L point.

(a) Find the appropriate linear combinations of plane waves which provide basis functions for the two lowest FCC L-point electronic states.
(b) Which states of the lower and upper energy levels in (a) are coupled by optical dipole transitions?
(c) Repeat parts (a) and (b) for the two lowest X point energy levels for the FCC empty lattice (i.e., the X_1, $X_{4'}$ and X_1, X_3, $X_{5'}$ levels).
(d) Compare your results to those for the simple cubic lattice.

12.3. (a) Considering the empty lattice model for the 2D hexagonal lattice (space group #17 $p6mm$), find the symmetries of the two lowest energy states at the Γ point ($k = 0$).
(b) Find the linear combination of plane waves that transform according to the irreducible representations in part (a).
(c) Repeat (a) and (b) for the lowest energy state at the M point shown in the Fig. 12.11.

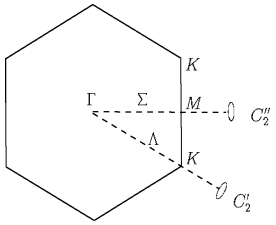

Fig. 12.11. Brillouin zone for the 2D triangular lattice

12.4. (a) Construct the character table for the group of the wave vector for the diamond structure at $k = 0$ using the classes given in Table 10.8 and check your results with Table C.17.

(b) Consider the effect of the symmetry operation $\{C_4|\tau_d\}$ for the diamond structure on the x_{11} and x_{12} basis functions in Table 12.8 to show that these basis functions stick together at the X point.
(c) Repeat (a) with the symmetry operation $\{C_4|\tau_d\}$ for the x_{31} and x_{32} basis functions in Table 12.8 to show that these basis functions come into the X point with zero slope.

12.5. Find the structure factor for the nonsymmorphic 3D graphite structure (see Problem 10.6) at a Δ point and at the A point in the Brillouin zone (see (12.34)) for the structure factor at the X point for diamond). Discuss the implication of your results on the electronic structure of 3D graphite.

12.6. Find the form of the $E(\boldsymbol{k})$ relation for the second level of the empty lattice for a BCC system and show how the degeneracy at $k = 0$ is lifted by application of a finite potential. What is the form of $E(\boldsymbol{k})$ for each of these cases, and compare your results to those for the $E(\boldsymbol{k})$ diagram for sodium (see Fig. 12.6(b)). To do this problem you will find Tables C.7 and C.8 of use.